PNAS RESEARCH ARTICLE | CELL BIOLOGY OPEN ACCESS

ALK fusion NSCLC oncogenes promote survival and inhibit NK cell responses via *SERPINB4* expression

Tzu-Po Chuang[a], Wei-Yun Lai[a,1], Jonatan L. Gabre[a,b,1], Dan E. Lind[a], Ganesh Umapathy[a], Abdulmalik A. Bokhari[a,2], Bengt Bergman[c], Linnea Kristenson[a], Fredrik B. Thorén[a], Anh Le[d], Robert C. Doebele[d], Jimmy Van den Eynden[b], Ruth H. Palmer[a,3], and Bengt Hallberg[a,3]

Edited by Joseph Schlessinger, Yale University, New Haven, CT; received October 4, 2022; accepted January 10, 2023

Anaplastic lymphoma kinase (ALK) fusion variants in Non-Small Cell Lung Cancer (NSCLC) consist of numerous dimerizing fusion partners. Retrospective investigations suggest that treatment benefit in response to ALK tyrosine kinase inhibitors (TKIs) differs dependent on the fusion variant present in the patient tumor. Therefore, understanding the oncogenic signaling networks driven by different ALK fusion variants is important. To do this, we developed controlled inducible cell models expressing either Echinoderm Microtubule Associated Protein Like 4 (EML4)-ALK-V1, EML4-ALK-V3, Kinesin Family Member 5B (KIF5B)-ALK, or TRK-fused gene (TFG)-ALK and investigated their transcriptomic and proteomic responses to ALK activity modulation together with patient-derived ALK-positive NSCLC cell lines. This allowed identification of both common and isoform-specific responses downstream of these four ALK fusions. An inflammatory signature that included upregulation of the Serpin B4 serine protease inhibitor was observed in both ALK fusion inducible and patient-derived cells. We show that Signal transducer and activator of transcription 3 (STAT3), Nuclear Factor Kappa B (NF-κB) and Activator protein 1 (AP1) are major transcriptional regulators of *SERPINB4* downstream of ALK fusions. Upregulation of *SERPINB4* promotes survival and inhibits natural killer cell-mediated cytotoxicity, which has potential for therapeutic impact targeting the immune response together with ALK TKIs in NSCLC.

non-small cell lung cancer | anaplastic lymphoma kinase | ALK fusion | NGS | phosphoprofiling

Significance

In this work, we have developed a highly controlled non-tumorigenic human bronchial epithelial cell system expressing four ALK fusions found in NSCLC. Employing RNA-seq and phosphoproteomics, we identify both common and isoform-specific differentially expressed genes and phosphorylated proteins downstream of these four ALK fusions. Further, we show that ALK fusions drive an inflammatory expression signature, resulting in increased Serpin B4 levels that result in inhibition of cytotoxic natural killer cell-induced cell death. Our study identifies a novel cell survival mechanism modulated by Serpin B4 downstream of ALK fusion oncogenes in NSCLC. This finding provides a potential therapeutic axis allowing targeting of the immune response together with ALK TKIs in NSCLC.

Oncogenic ALK fusions were identified in Non-Small Cell Lung Cancer (NSCLC) in 2007, in both tumor material and cell lines (1, 2). ALK fusions, resulting from chromosomal translocation events, are recognized as drivers in approximately 5% of NSCLC (3). ALK fusions generally contain exons 20 to 29 of *ALK*, which encode the entire C-terminal kinase domain. The N-terminal portions of the ALK fusions in NSCLC consist of numerous fusion partners, such as EML4, TFG, and KIF5B, among more than 90 ALK fusion partners that have been described (3). The most frequently observed ALK fusion is EML4-ALK which represents more than 85% of ALK-positive NSCLC cases, where EML4-ALK variants 1, 2, and 3 account for 43%, 6%, and 40% of cases, respectively (4, 5). These ALK fusion partners dimerize and activate the ALK kinase domain and also determine "when and where" the fusion protein is expressed (3). Very little is known about differential downstream targets of the ALK fusion proteins, but these likely include an array of signaling pathway components, reflecting spatial and temporal restraints determined by the respective fusion partners (6).

Lately, retrospective analyses of patients with NSCLC EML4-ALK fusions have suggested that the degree of treatment benefit in response to ALK tyrosine kinase inhibitors (TKIs) might be dependent on the particular ALK fusion variant expressed, reviewed in ref. 3. This includes an initial retrospective report of improved overall response rate upon treatment with crizotinib in EML4-ALK-V1 patients compared to the non-V1 variant group (7). Christopoulos and coworkers reported that patients with EML4-ALK-V3-driven tumors with and without *TP53* mutations had more metastatic sites and decreased progression-free survival compared with other ALK-driven variants (5, 8, 9). Finally, results from the ALTA-1L phase 3 clinical trial revealed that patients harboring EML4-ALK-V3 exhibit worse progression-free survival and overall responsive rate when compared with patients with EML4-ALK-V1, irrespective of treatment with crizotinib or brigatinib (10).

The *SERPIN* gene family consists of 36 protein coding genes as well as several pseudogenes (11). Serpins are protease inhibitors with broad biological functions. The clade B Serpin subfamily has a predominantly intracellular distribution, and 10 out of 13 genes are clustered at chromosome 18q21.3 (12, 13). *SERPINB3* and *B4* are highly homologous at the nucleotide and amino acid level and are believed to have arisen by gene duplication (13). Although their in vivo functions remain largely unclear, Serpin B3 has been shown to inhibit papain-like cysteine proteases, while Serpin B4 inhibits chymotrypsin-like serine

Author contributions: T.-P.C., F.B.T., R.C.D., R.H.P., and B.H. designed research; T.-P.C., W.-Y.L., D.E.L., G.U., A.A.B., B.B., L.K., and A.L. performed research; J.L.G., J.V.d.E., R.H.P., and B.H. analyzed data; and T.-P.C., R.H.P., and B.H. wrote the paper.

The authors declare no competing interest.

This article is a PNAS Direct Submission.

Copyright © 2023 the Author(s). Published by PNAS. This open access article is distributed under Creative Commons Attribution-NonCommercial-NoDerivatives License 4.0 (CC BY-NC-ND).

[1]W.-Y.L. and J.L.G. contributed equally to this work.

[2]Present address: Department of Biomedical Sciences, College of Veterinary Medicine, King Faisal University, Al-Ahsa 31982, Saudi Arabia.

[3]To whom correspondence may be addressed. Email: ruth.palmer@gu.se or bengt.hallberg@gu.se.

This article contains supporting information online at https://www.pnas.org/lookup/suppl/doi:10.1073/pnas.2216479120/-/DCSupplemental.

Published February 15, 2023.

proteases such as Granzyme M with its specific reactive center loop (13, 14). Granzymes are key cytotoxic effector molecules released by CD8$^+$ T cells and natural killer (NK) cells upon recognition of malignant cells. Like other members of the family, Granzyme M can efficiently trigger cell death in tumor cells (15). Interestingly, elevated levels of Serpin B3 and B4 have been noted in NSCLC, where they are associated with poor survival (16). Furthermore, inactivating mutations in *SERPINB3* and *SERPINB4* are associated with improved survival after anti-CTLA4 immunotherapy in patients with melanoma (17).

Currently, treatment of ALK-driven NSCLC is decided without considering the fusion partner involved, although these different fusion partners are suspected to affect pretreatment clinical characteristics, disease responsiveness to target therapies, and later arising acquired resistance (18). We have developed an experimental approach to investigate differential activity of ALK fusion variants expressed in NSCLC with focus on EML4-ALK variants 1 (V1) and 3 (V3), KIF5B-ALK and TFG-ALK. We identify downstream signaling components regulated by these ALK fusion variants, crosstalk, and adaptive responses in NSCLC cell lines, employing both cell lines engineered to express inducible ALK fusions as well as patient-derived cell lines. Analyses of phosphoproteomic and transcriptional responses to ALK TKI treatment allowed us to generate signatures reflecting ALK signaling events from the different ALK fusions. One previously unidentified target is Serpin B4, which is robustly expressed in both EML4-ALK (V3) and TFG-ALK expressing cells. Phosphoproteomics identified NF-κB as a regulator of *SERPINB4* expression in response to ALK fusion activity, and NF-κB inhibition decreased expression of Serpin B4 at both protein and mRNA levels. Further, both STAT3 and AP1 regulate Serpin B4 protein expression. Finally, we show that EML4-ALK-V3 and TFG-ALK-driven Serpin B4 expression is able to rescue cells from NK cell-mediated cytotoxicity. Our results indicate that Serpin B4 expression may represent an important factor in the poor prognosis of patients diagnosed with EML4-ALK-V3 and identifies an avenue for therapeutic intervention.

Results

Generation and Characterization of Inducible Cell Lines Expressing EML4-ALK-V1, EML4-ALK-V3, KIF5B-ALK, and TFG-ALK Fusion Variants. To investigate ALK fusion variants in NSCLC in an experimentally controlled manner, we selected four variants with different fusion partners for in-depth investigation (Fig. 1*A*). These were the coiled-coil domain containing EML4-ALK-V1 and -V3, which were selected as they account for 70 to 80% of all EML4-ALK-positive NSCLC cases (5), KIF5B-ALK, which harbors multiple coiled-coil oligomerization domains and TFG-

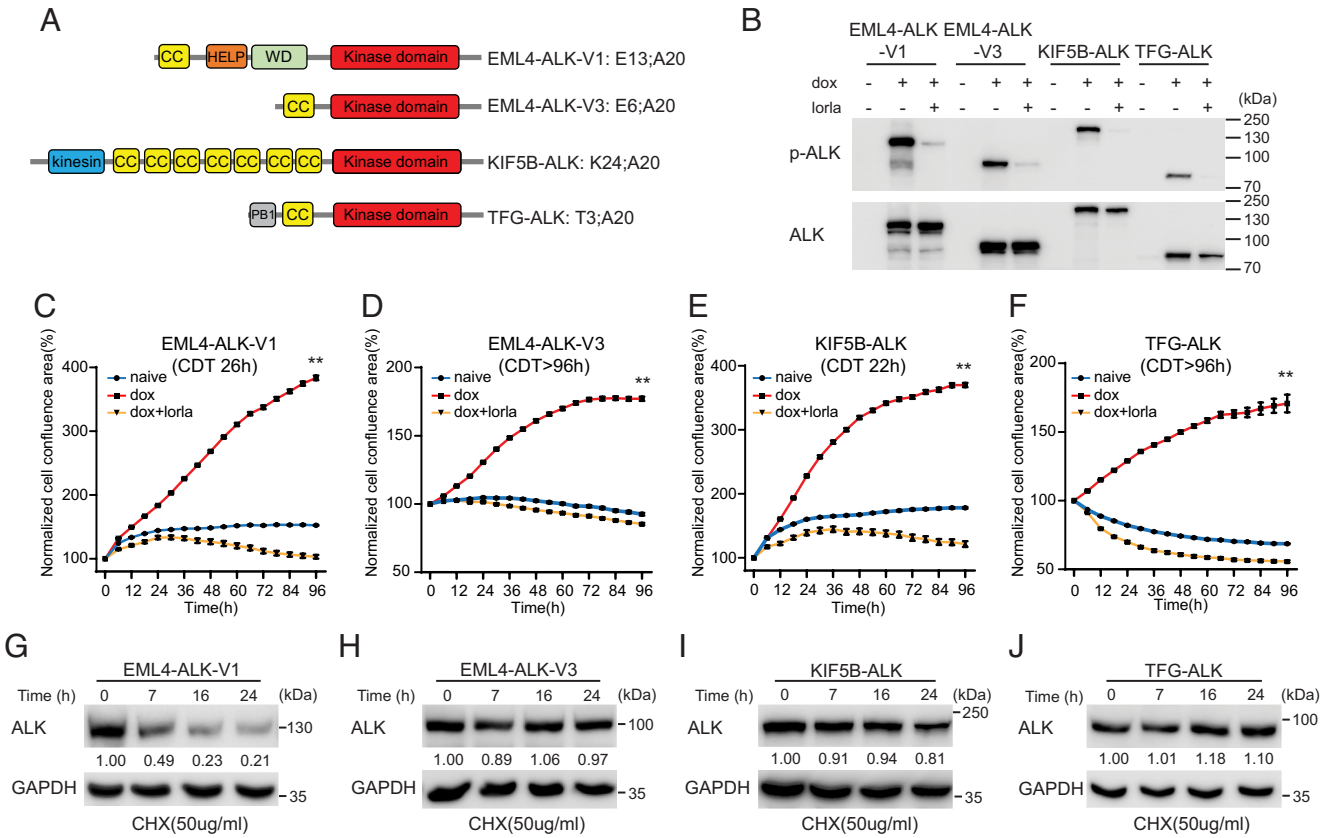

Fig. 1. Characterization of NL20 cells expressing ALK NSCLC fusions. (*A*) Schematic representation of ALK fusion proteins investigated in this study. The breakpoint located at exon 20 in ALK is identical in all four ALK fusions. EML4-ALK-V1 (E13; A20) and V3 (E6; A20) harbor exons 1 to 13 and 1 to 6 of EML4, respectively; KIF5B-ALK (K24; A20) and TFG-ALK (T3; A20) contain exons 1 to 24 of KIF5B and exons 1 to 3 of TFG, respectively, fused to exon 20 of ALK. Protein domains are indicated as: coiled coil (CC, yellow), hydrophobic motif in EML proteins (HELP) (orange), tryptophan-aspartic acid repeat domain (WD) (green), ALK kinase domain (red), kinesin (blue), and PB1 (gray). (*B*) ALK fusions were induced in NL20-ALK cells with doxycycline (dox) in the presence or absence of lorlatinib (lorla, 30 nM), and lysates immunoblotted with pY1278-ALK and pan-ALK as indicated. PhosphoY1278-ALK (p-ALK) was employed as readout of ALK inhibition. (*C–F*) NL20-ALK cells were treated with DMSO (blue), doxycycline (red), or doxycycline plus lorlatinib 30 nM (orange). Cell confluence was monitored using an IncuCyte® Live Cell Analysis system. Data points represent mean ± SEM of normalized cell confluence conducted in triplicate. Cell doubling time of individual cell lines is indicated (**$P < 0.01$, two-tailed paired *t* test). One typical experiment of three independent experiments is shown. (*G–J*) NL20-ALK stable cell lines were treated with cycloheximide (CHX) for 7, 16 and 24 h, and resulting lysates immunoblotted for ALK and Glyceraldehyde-3-Phosphate Dehydrogenase (GAPDH). Quantification of ALK fusion protein levels compared to GAPDH control is depicted below each lane (n = 3, a representative result is shown).

ALK, which harbors one coiled-coil, which is important for dimerization (Fig. 1*A*) (2, 19–21).

Inducible clonal cell lines for each of the four ALK fusion variants were generated in the immortalized, non-tumorigenic NL20 cell line derived from human bronchial epithelium (CRL-2503, American Type Culture Collection (ATCC)) (Fig. 1*B*). ALK fusion expressing NL20 cells expressed active phosphorylated EML4-ALK-V1/EML4-ALK-V3/KIF5B-ALK/TFG-ALK in response to doxycycline, and this activity (pY1278-ALK) was inhibited in the presence of the ALK TKI lorlatinib. ALK fusion expression levels, sequence and downstream signaling activity, pAKT and pERK, were confirmed for three individual clones for each ALK fusion (Fig. 1*B* and *SI Appendix*, Fig. S1).

Having generated multiple inducible ALK fusion expressing NL20 cell clones expressing EML4-ALK-V1, EML4-ALK-V3, KIF5B-ALK, and TFG-ALK and confirmed ALK signaling activity, we proceeded to characterize differences in the different ALK fusion expressing cells. ALK fusion protein expression resulted in increased proliferation in the absence of serum relative to non-induced controls (Fig. 1 *C*–*F* and *SI Appendix*, Fig. S2). This increase in proliferation was abrogated on addition of ALK TKI (30 nM lorlatinib) (Fig. 1 *C*–*F* and *SI Appendix*, Fig. S2). Differences in proliferation rates were observed between EML4-ALK-V1, EML4-ALK-V3, KIF5B-ALK, and TFG-ALK expressing NL20 cells; EML4-ALK-V1 and KIF5B-ALK exhibited faster growth rates, with cell doubling times of 26 and 22 h, respectively, while EML4-ALK-V3 and TFG-ALK showed slower growth rates with doubling times of around 96 h (Fig. 1 *C*–*F*).

Global tyrosine phosphorylation on induction of either EML4-ALK-V1, EML4-ALK-V3, KIF5B-ALK, or TFG-ALK was also investigated over an 8 h time-course confirming increased tyrosine phosphorylation of i) the ALK fusion variant in question and ii) additional cellular proteins (*SI Appendix*, Fig. S3). We also investigated kinase activity of the different ALK fusion variants (*SI Appendix*, Fig. S4). We observed that KIF5B-ALK exhibits the highest level of kinase activity, whereas TFG-ALK exhibits relatively low kinase activity in in vitro kinase assays, which is in agreement with earlier reports that KIF5B-ALK fusions show increased kinase activity when compared with ALK fusions found in NSCLC (22).

Since previous reports have described differences in protein stability of the EML4-ALK variants (22, 23), we examined EML4-ALK-V1, EML4-ALK-V3, KIF5B-ALK, and TFG-ALK fusion protein stability. ALK fusion stability was examined over 24 h in the presence of cycloheximide to inhibit de novo protein synthesis. In agreement with previous reports (22, 23), we observed that EML4-ALK-V1 has a high turnover as indicated by a decrease in fusion protein levels (Fig. 1*G*). We also observed that KIF5B was slightly instable (Fig. 1*I*), while both EML4-ALK-V3 and TFG-ALK fusions were relatively stable(Fig. 1 *H* and *J*).

Taken together, these data confirm the establishment of a controlled system in a lung epithelial cell line, with which to dissect the molecular properties of the EML4-ALK-V1, EML4-ALK-V3, KIF5B-ALK, and TFG-ALK NSCLC oncogenic variants.

ALK Fusions Induce Overexpression of *SERPINB* Genes. We induced expression of either EML4-ALK-V1, EML4-ALK-V3, KIF5B-ALK, or TFG-ALK fusions and performed RNA-sequencing (RNA-seq) differential expression (DE) analysis at 24 h after fusion induction (Fig. 2*A*). As expected, *ALK* and the respective fusion protein was up-regulated in all cells 24 h after induction (Fig. 2*B* and *SI Appendix*, Fig. S5). Fusion induction resulted in a DE response of 1,128, 887, 1,707, and 553 genes for EML4-ALK-V1, EML4-ALK-V3, KIF5B-ALK, or TFG-ALK, respectively, with 205 genes DE by all four fusions (Fig. 2*A* and *SI Appendix*, Table S1). These genes were strongly enriched for Tumor Necrosis Factor-Alpha (TNF-α) signaling via NF-κB (P_{adj} = 4.5e−14) and Interleukin-2 (IL2)-Signal transducer and activator of transcription 5 (STAT5) signaling (P_{adj} = 2.0e−07) as observed from a Hallmark gene set enrichment analysis (GSEA) (Fig. 2*C*). These gene sets include several genes of the *SERPINB* family, including *SERPINB2* and *SERPINB8*, and a strong upregulation of other *SERPINB* genes (*SERPINB3*, *SERPINB4*, *SERPINB7*, *SERPINB11*) was observed after ALK fusion induction (Fig. 2*B*). The strongest upregulation was observed for *SERPINB4* in EML4-ALK-V3 (log2FoldChange(FC) = 13.3) and TFG-ALK (log2FC = 12.0) cells, which was also validated at the protein level (Fig. 2 *B*, *D*, and *E*). *SERPINB3* and *SERPINB11* showed strikingly similar DE responses to *SERPINB4,* and, remarkably, an opposite response was observed after TKI treatment of ALK-positive NSCLC patient-derived cell lines carrying the EML4-ALK-V3 fusion (YU1077 and CUTO29 cells), but not after similar treatment with cells carrying the EML4-ALK-V1 fusion (CUTO8 and CUTO9 cells; Fig. 2*F* and *SI Appendix*, Fig. S5). Further, data from the H2228 NSCLC line (expressing EML4-ALK-V3) and H3122 (expressing EML4-ALK-V1) show similar results as our patient-derived cell lines (Fig. 2*F* and *SI Appendix*, Fig. S5). A similar, but weaker, mirrored response was observed for *SERPINB2*, *SERPINB7*, *SERPINB8*, *SERPINB10,* and *SERPINB13*. Interestingly, the *SERPINB* family members clustered at chromosome 18q21 are all up-regulated on induction of EML4-ALK-V3 protein expression, and conversely, EML4-ALK-V3 expressing YU1077 and CUTO29 cells exhibit reduced levels of many of these on treatment with lorlatinib (Fig. 2*F*).

Phosphoprofiling of Signaling Events Downstream of NSCLC ALK Fusions. To determine the effects of the different ALK fusions on cellular phosphorylation signaling activity, we performed a phosphoproteomic analysis on NL20 cells after induction of EML4-ALK-V1, EML4-ALK-V3, KIF5B-ALK, and TFG-ALK fusions, both in control conditions and after treatment with lorlatinib (Fig. 3*A*). Differential phosphorylation (DP) in response to lorlatinib was determined between ALK fusion expressing cell lines and controls. Initial in-depth analysis focused on the EML4-ALK-V1 and EML4-ALK-V3 fusions, which represent the majority of NSCLC ALK fusions. A strong hyperphosphorylation response was observed after fusion induction in EML4-ALK-V3 cells (282 sites hyperphosphorylated), but not for the other fusions (41 to 78 sites hyperphosphorylated; Fig. 3 *B* and *C* and *SI Appendix*, Fig. S6). This response included ALK at Y1078 (logFC = 11), ALK at Y1359 (logFC = 7.5), NF-κB2 at Y77 (logFC = 7.7), and STAT3 at Y705 (logFC = 2.8) and was sensitive to lorlatinib treatment (only 67/282 sites hyperphosphorylated after treatment), suggesting ALK dependency. While Y705 phosphorylation of STAT3 has been well-documented downstream of oncogenic ALK (25–29), the striking tyrosine phosphorylation of NF-κB1 and NF-κB2, which is supported by the NF-κB signature identified in our RNA-seq analysis (Fig. 2*C*), has not previously been reported. Tyrosine kinase dependency was further confirmed by the strong enrichment for tyrosines in these hyperphosphorylated sites (92.9% vs. 18.7% in non-hyperphosphorylated sites in EML4-ALK-V3; P = 5.0e−174; Fig. 3 *D* and *E*). Lorlatinib treatment again resulted in a decrease in this proportion (Fig. 3*E*). Inspection of the ALK fusion portion resulted in identification of all previously identified phosphotyrosine sites, including the three tyrosines, Y1278, Y1282, and Y1283, that are located in the ALK activation loop and have been shown to be essential for

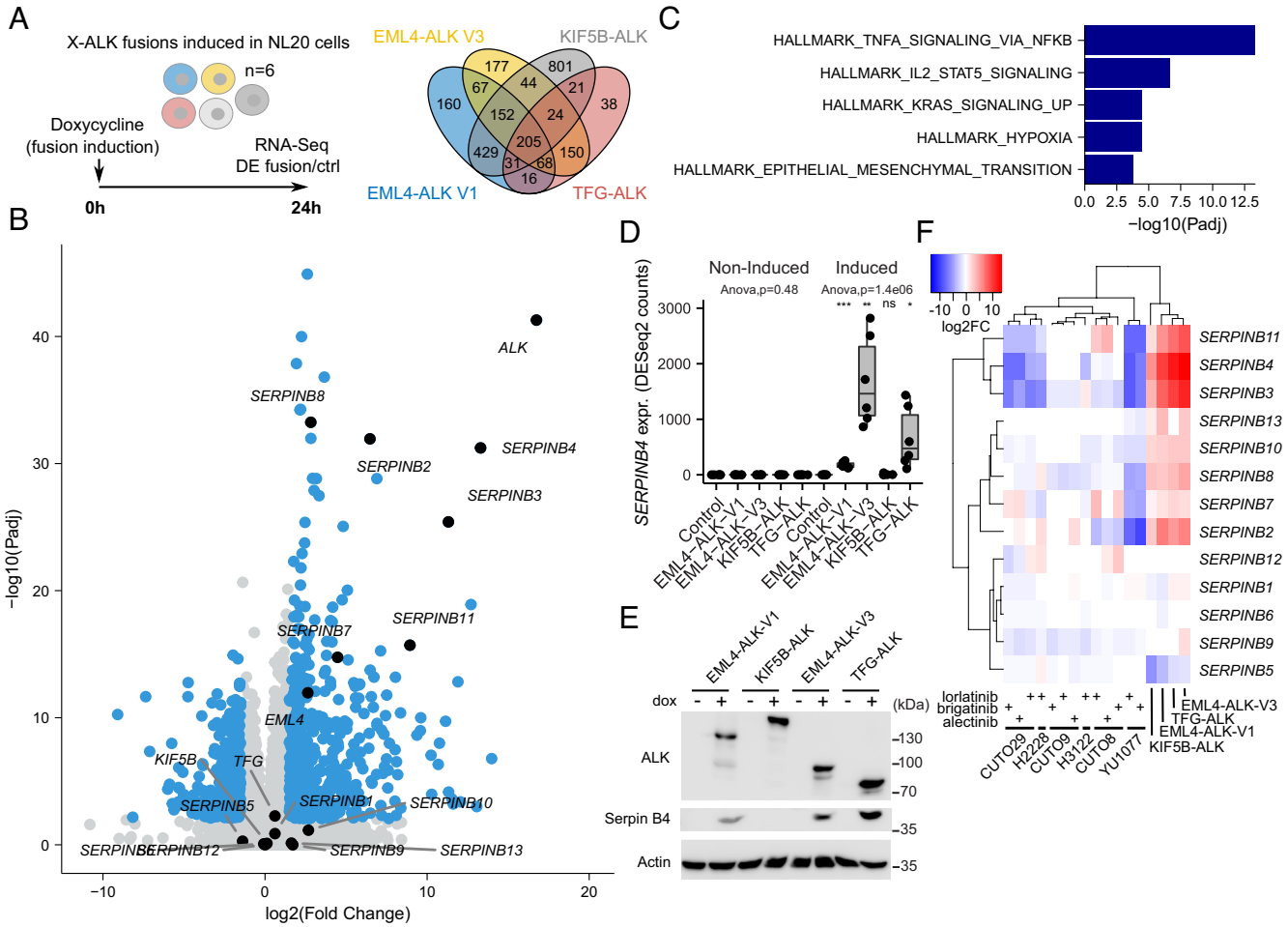

Fig. 2. Transcriptomic response to ALK fusion expression in NL20 cells. (*A*) ALK fusions were independently induced in NL20 cells, and RNA-seq-based DE with control cells was determined 24 h after fusion induction with doxycycline (dox). Venn diagram showing the number of DE genes (log2FC +/−1.5 at 1% False Discovery Rate (FDR), using a hyperbolic threshold) for each fusion as indicated. n = 6, RNA-seq analysis from three independent clones per variant performed in duplicate. See *SI Appendix*, Table S1 for detailed results. (*B*) Volcano plot showing DE response to EML4-ALK-V3 fusion induction. DE genes indicated in blue with genes discussed in main text indicated and labeled in black. (*C*) Hallmark GSEA results in 205 common genes that were DE for all four ALK fusions. GSEA was performed using Fisher's exact test. Bars represent adjusted *P*-values (−log10 scale) for enriched gene sets at 5% FDR. (*D*) Box plot showing *SERPINB4* expression for all four non-induced and dox-induced ALK fusions and control cells as indicated. ANOVA performed independently on non-induced and induced conditions. Asterisks indicating significance when comparing fusions to Ctrl cells (Student's *t* test). NS, non-significant; $*P < 0.05$; $**P < 0.01$; $***P < 0.001$. (*E*) Immunoblot validation of Serpin B4 protein expression before and after fusion induction as indicated. (*F*) Heatmap showing DE log2FC values (color scale at top left) of all 13 *SERPINB* genes for the four ALK fusions as well as six ALK-positive patient-derived cell lines (CUTO29, H2228, CUTO9, H3122, CUTO8, YU1077) treated with three different ALK inhibitors as indicated. Dendrograms indicate hierarchical clustering results. RNA-seq data generated from H2228 and H3122 as well as from the recent patient-derived CUTO8, 9, 29, and YU1077 cells (24).

auto-activation and transforming activity (30, 31). We also noted differential ALK phosphorylation at Y1359, which was decreased in response to lorlatinib treatment after fusion induction (logFC: −2.2 and −2.2 in −V1 and −V3, respectively), but was unchanged in TFG-ALK (Fig. 3*D*). Y1359 is located in the C-lobe of the ALK kinase domain within the alpha-H-helix and presents a structurally accessible phosphorylation site of currently unknown functional consequence (32, 33). Intriguingly, phosphorylation of Y1131 also showed differential lorlatinib sensitivity between the ALK fusion variants. Further, significant lorlatinib sensitivity was observed in the identified phosphorylation sites of proteins containing Phosphotyrosine-binding domain (PTB) and Src Homology 2 (SH2) phosphotyrosine binding domains, which are putative downstream targets of the ALK fusions (*SI Appendix*, Fig. S7 *A* and *B*). Phosphorylation in these proteins was indeed significantly reduced on lorlatinib treatment with stronger responses for EML4-ALK-V3 than EML4-ALK-V1, in keeping with our findings (*SI Appendix*, Fig. S7 *A* and *B*). We also noted differences in the phosphorylation of these phosphotyrosine binding domains containing proteins, where EML4-ALK-V1 appears to preferentially engage CT10 regulator of kinase-like (CRKL), while EML4-ALK-V3 appears to preferentially engage CT10 regulator of kinase (CRK) (*SI Appendix*, Fig. S7 *C*). Overall, our phosphoproteomics analysis suggests that there are differences in downstream signaling output, which may reflect differences in the phosphorylation of the ALK fusion itself as well as the subcellular localization of the ALK fusion in question.

EML4-ALK V3 and TFG-ALK Induce *SERPINB4* Expression via STAT3, NF-κB, and AP1. The identification of phosphorylated STAT3, Finkel-Biskis-Jinkins osteosarcoma-like 1 (FOSL1), and NF-κB in our phosphoproteomics analysis, together with the upregulation of *SERPINB4* in NL20 cells expressing the various ALK fusions, led us to further investigate *SERPINB4* in the context of ALK fusions and NSCLC. *SERPINB4* and *B3* have been reported to be STAT3 transcriptional targets (34), and a recent report has described a transcriptional signature driving an inflammatory regulatory network in human cancers that is jointly regulated by NF-κB, STAT3, and AP1 (35). In agreement, we observed that this NF-κB, STAT3, and AP1 mediated inflammatory

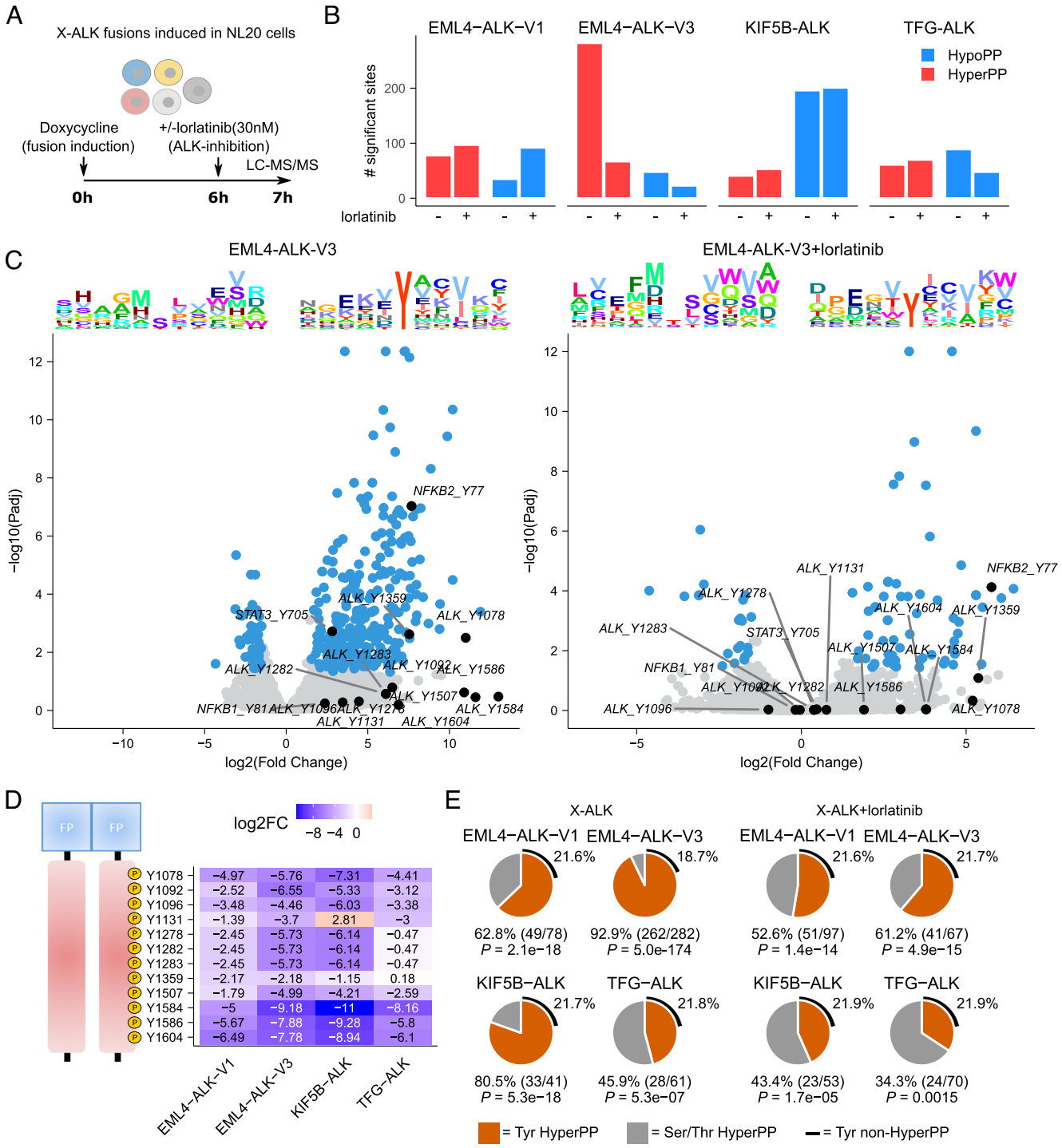

Fig. 3. Lorlatinib-dependent phosphoproteomic response to ALK fusion induction. (*A*) DP between the four different ALK fusions and control NL20 cells was determined 7 h after fusion induction with doxycycline (dox). Cells were treated with lorlatinib 6 h after fusion induction as indicated. (*B*) Bar plot indicating the number of hyper- and hypophosphorylated sites (log2FC +/−1.5 at 5% FDR, using a hyperbolic threshold) in control and lorlatinib treatment conditions as indicated. (*C*) Volcano plots showing DP response in control (*Left*) and lorlatinib-treated (*Right*) EML4-ALK-V3 cells. DP sites indicated in blue with sites discussed in main text indicated and labeled in black. Sequence logo plots showing position-specific enrichment ±5 amino acids centered around the phosphorylation site for hypo- and hyperphosphorylated sites shown on top. (*D*) Heatmap showing DP (logFC values) between lorlatinib-treated and untreated fusions for all ALK tyrosine sites. Position in ALK indicated (*Left*). (*E*) Pie charts showing the proportion of tyrosine motifs in hyperphosphorylated sites in cells expressing ALK fusions in the presence or absence of lorlatinib. *P*-values calculated using Fisher's exact test, estimating likelihood of overrepresentation of tyrosines in hyperphosphorylated sites.

signature was indeed significantly enriched in cells expressing the EML4-ALK-V1, EML4-ALK-V3, and TFG-ALK variants, but not the KIF5B-ALK fusion variant (Fig. 4*A*). To validate this, we measured pY705-STAT3, pS265-FOSL1, and pS63-c-JUN phosphorylation in NL20-ALK fusion cell lines, noting that all three phosphorylation sites were robustly increased on ALK fusion expression and dephosphorylated upon treatment with lorlatinib, indicating that these phosphorylation events are dependent on ALK activity, in agreement with our phosphoproteomics datasets (Fig. 4 *B* and *C* and *SI Appendix*, Table S2). We next examined NF-

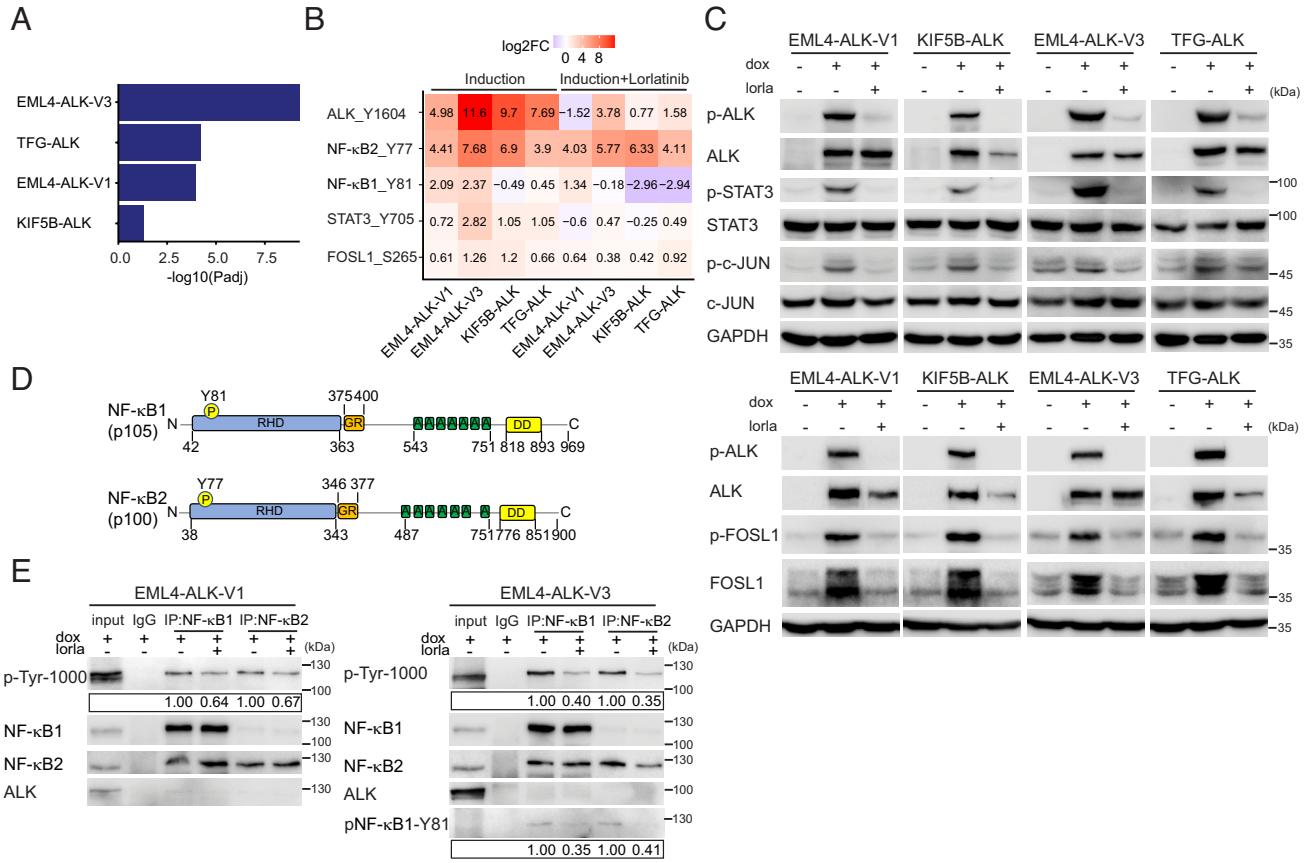

Fig. 4. Activation of STAT3, AP1 and NF-κB downstream of NSCLC ALK fusions. (*A*) Gene set enrichment for 27 inflammatory response genes (35) in DE genes in ALK fusions as indicated. GSEA was performed using Fisher's exact test. Bars represent P_{adj} values (−log10 scale). (*B*) Heatmap of DP logFC values (comparing each fusion to control cells) at ALK-Y1604, NF-κB2-Y77, NF-κB1-Y81, STAT3-Y705, and FOSL1-S265, in the presence (*Right*) or absence (*Left*) of lorlatinib. (*C*) ALK fusions were induced in NL20-ALK cells with doxycycline (dox) in the presence or absence of lorlatinib (lorla, 30 nM), and lysates immunoblotted with pY1278-ALK, pan-ALK, pY705-STAT3, pan-STAT3, pS265-FOSL1, FOSL1, pS63-c-JUN, pan-c-JUN, and GAPDH as indicated. Phospho-ALK (pY1278-ALK) was employed as readout of ALK inhibition. (*D*) Schematic representation of NF-κB1 and NF-κB2 proteins and phosphotyrosine sites identified in this study. Protein functional domains are indicated as: Rel-homology domain (RHD, blue), glycine-rich region (GR, orange), ankyrin repeat (A, green), and death domain (DD, yellow). (*E*) NF-κB1/NF-κB2 were immunoprecipitated from EML4-ALK-V1 or EML4-ALK-V3 expressing NL20 cells, in the presence or absence of lorlatinb (lorla), with NF-κB-specific antibodies as indicated, followed by immunoblotting with anti-p-Tyr-1000, NF-κB1, NF-κB2, ALK, and phosphor-specific NF-κB-Y81. Blots are representative of three different experiments. Quantification of phosphotyrosine levels is shown in box. n = 3, a representative result is shown.

κB1 and NF-κB2, which were phosphorylated on Y81 (NF-κB1) and Y77 (NF-κB2), sites located in the Rel-homology domain that are conserved in mouse and rat orthologues (Fig. 4*D*). Since no phosphospecific antibodies to these tyrosine phosphorylation sites in NF-κB exist, we developed antibodies against these sites. This resulted in generation of a phospho-NF-κB1-Y81 antibody. We employed immunoprecipitation with either NF-κB1 or NF-κB2 antibodies, followed by anti-PY and phospho-NF-κB1-Y81 immunoblotting to confirm phosphorylation in response to ALK fusion oncogene activity and reduction of tyrosine phosphorylation on lorlatinib treatment (Fig. 4*E*). Thus, all three components NF-κB, STAT3, and the AP1 component FOSL1 appear to be robustly activated in response to ALK expression and activity.

Examination of the promoter region of *SERPINB4* identifies sites for NF-κB, STAT3, and AP1 (Fig. 5*A*), suggesting that they may act in concert to drive *SERPINB4* expression. Indeed, stimulation of the NL20 parental cell lines with TNF-α resulted in a dose-dependent activation of STAT3, as well as NF-κB (p52) accumulation that correlated with an increase in *SERPINB4* expression (Fig. 5*B*) (36). To further investigate the role of STAT3 and NF-κB in *SERPINB4* expression, we first manipulated STAT3 in ALK fusion expressing cells. siRNA silencing of STAT3 resulted in the loss of Serpin B4 protein in cells expressing either EML4-ALK-V1, EML4-ALK-V3, or TFG-ALK (Fig. 5*C*). Moreover, inhibition of NF-κB with the 4-Methyl-N1-(3-phenyl-propyl)-benzene-1,2-diamine (JSH-23) inhibitor (37) resulted in decreased transcription of *SERPINB4* in EML4-ALK-V1, EML4-ALK-V3, or TFG-ALK expressing cells (Fig. 5*D*). Likewise, inhibition of AP1 employing two different inhibitors which inhibit either JNK (CC-930) or AP1 binding (T-5224) resulted in decreased transcription of *SERPINB4* in all ALK fusion variants (Fig. 5*E*). In agreement with our earlier RNA-seq analysis, basal levels of *SERPINB4* mRNA expression were different in the various ALK fusion cell lines, with very low levels of *SERPINB4* mRNA detected in EML4-ALK-V1 and KIF5B-ALK fusion expressing cells. As the NL20 parental cell line is a non-tumorigenic cell line, we investigated the transforming potential of EML4-ALK-V1 vs. -V3. Subcutaneous injection of doxycycline-induced NL20 cells expressing either EML4-ALK-V1 or -V3 in BALB/cAnNRj-Foxn1nu mice, fed +/− doxycycline, identified a faster tumor take for EML4-ALK-V3 (4 out of 5), than for EML4-ALK-V1 (5 out of 5), with an average tumor take of 6 to 7 wk compared with 12 wk (Fig. 5*F*), respectively. In the absence of doxycycline, neither EML4-ALK-V1 nor -V3 resulted in tumor formation (Fig. 5*F*). Tumors from animals harboring either EML4-ALK-V1 or -V3 were analyzed for expression of phosphorylated and pan-ALK, STAT3, AKT, Extracellular Signal-Regulated Kinase (ERK), or

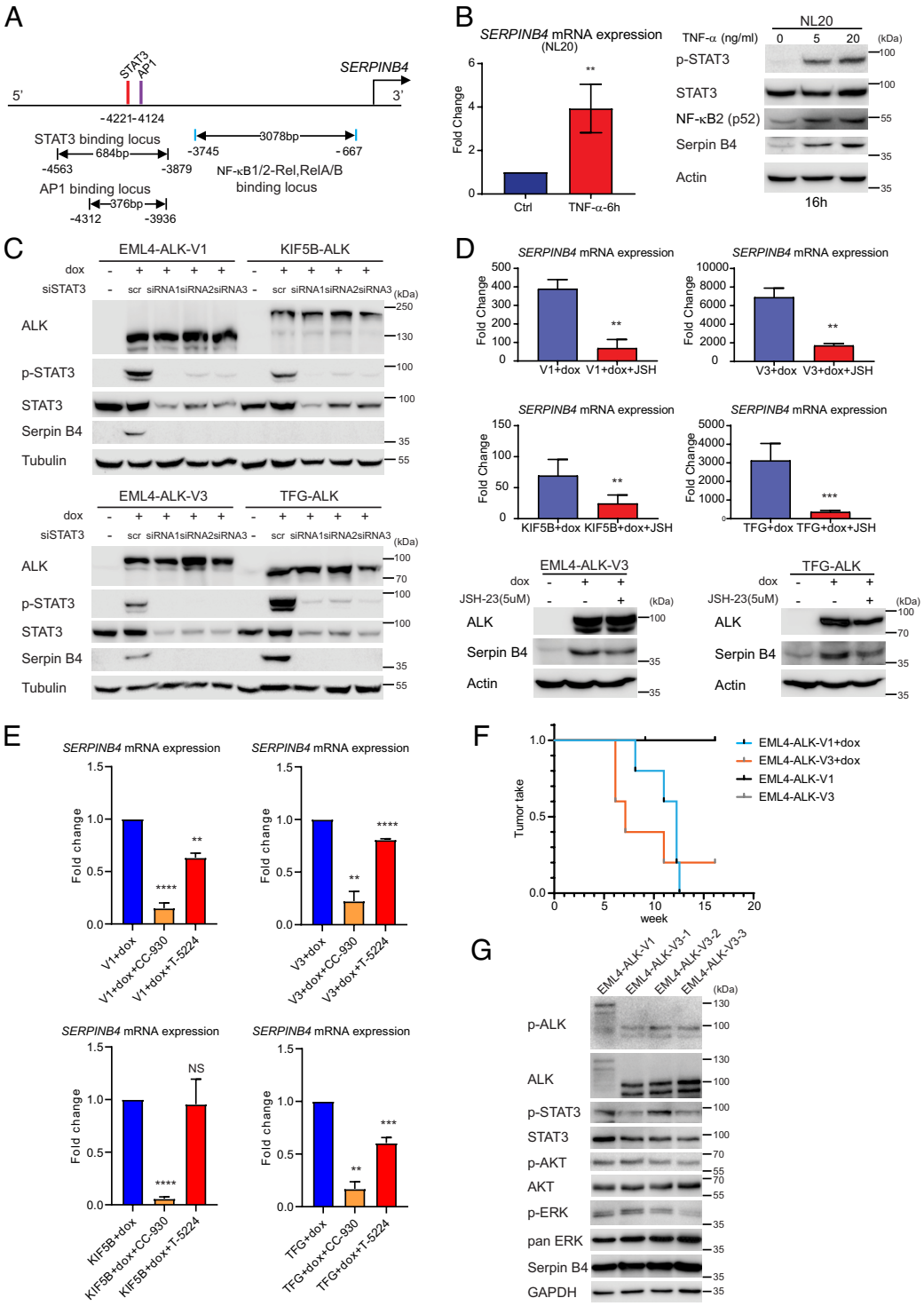

Fig. 5. NSCLC ALK fusions drive *SERPINB4* expression via STAT3 and NF-κB. (*A*) Schematic representation of the *SERPINB4* promoter region. Red bars show predicted STAT3 binding motifs, and purple and blue bars indicate predicted AP1 and NF-κB binding sites, respectively. (*B*) TNF-α induces *SERPINB4* expression in NL20 cells. NL20 cells were treated with TNF-α for 6 h followed by qRT-PCR on total RNA. (*Left*) Fold change *SERPINB4* mRNA expression normalized to untreated controls (Ctrl), (n = 3; $^{**}P < 0.01$; two-tailed paired *t* test). (*Right*) NL20 cells were treated with TNF-α (0, 5, 20 ng/mL) for 16 h, and lysates subjected to immunoblotting analysis with pY705-STAT3, pan-STAT3, NF-κB2, Serpin B4, and Actin antibodies as indicated. (*C*) NL20-ALK cells were transfected with either control siRNA (scr) or siRNAs (1 to 3) targeting STAT3 upon doxycycline (dox) addition. Resulting cell lysates were immunoblotted with pan-ALK, pY705-STAT3, pan-STAT3, Serpin B4, and Tubulin antibodies as indicated. (*D*) NL20-ALK cells treated with JSH-23 (5 μM) for 24 h upon doxycycline (dox) addition followed by either qPCR or immunoblotting analysis. Fold change *SERPINB4* mRNA expression was normalized to untreated (no dox) controls and data presented as mean ± SD (n = 3; $^{**}P < 0.01$; two-tailed paired *t* test). JSH-23-treated and control cell lysates were subjected to immunoblotting analysis with ALK, Serpin B4, and Actin antibodies as indicated. (*E*) NL20-ALK cells treated with CC-930 (10 μM) or T-5224 (10 μM) for 24 h upon doxycycline (dox) addition followed by qPCR analysis. Fold change *SERPINB4* mRNA expression was normalized to untreated controls and data presented as mean ± SD (n = 3; NS, non-significant; $^{**}P < 0.01$; $^{***}P < 0.001$; $^{****}P < 0.0001$; two-tailed paired *t* test. (*F*) Doxycycline-induced NL20-EML4-ALK-V1 or NL20-EML4-ALK-V3 cells (2.5×10^6 per injection) were injected into female athymic nude mice in the presence or absence of doxycycline (dox, 625 mg/kg delivered in feed, n = 5) as indicated. Animals in each treatment group were maintained for 15 wk and tumor development monitored. Data are presented as tumor incidence over time. Kaplan–Meier analysis with Mantel–Cox log-rank test and Bonferroni-corrected threshold. $P = 0.0044$ for V1 vs. V1+dox, $P = 0.0128$ for V3 vs. V3+dox and $P = 0.610$ for V1+dox vs. V3+dox. (*G*) Tumors from EML4-ALK-V1 (one tumor sample) and EML4-ALK-V3 (three tumor samples) were harvested, and homogenized cell lysates subjected to immunoblotting analysis with pY1278-ALK, pan-ALK, pY705-STAT3, pan-STAT3, pS473-AKT, pan-Akt, pT202/Y204-ERK1/2, pan-ERK, Serpin B4, and GAPDH antibodies as indicated.

expression of Serpin B4. All resected tumors sections showed expression of the expected EML4-ALK fusions as well as downstream signaling proteins (Fig. 5*G*). Taken together, these results show that active ALK fusion variants potently activate STAT3/NF-κB/AP1 leading to the upregulation of *SERPINB4* expression.

Serpin B4 Protects NL20-ALK Cells against NK Cell Cytotoxicity. Increased *SERPINB4* expression has been associated with a more aggressive phenotype in lung cancer (13), and several groups have reported a role for Serpin B4 in preventing apoptosis (14, 38). To examine this further, we monitored NL20 parental cells overexpressing Serpin B4 (Fig. 6*A*). We observed a significant decrease of apoptosis (caspase-3/7 positive cells) when Serpin B4 was overexpressed (Fig. 6*A*). Overexpression of Serpin B4 decreased phosphorylation of p38 and c-JUN pathway components and downstream substrates, such as Activating transcription factor 2 (ATF2) and inactivated ERK1/2 signaling (39, 40) (Fig. 6*B*). c-JUN and p38 are stress-activated protein kinases that are activated in response to endogenous and exogenous stress stimuli (39). Their effect is generally anti-proliferative and proapoptotic, but dependent on cellular context they can be involved in tumorigenesis (41). Increased cell survival was observed in Serpin B4 expressing NL20 cells challenged with either TNF-α or with hydrogen peroxide (H_2O_2), supporting a role for Serpin B4 in the suppression of apoptosis (Fig. 6 *C* and *D*) (39, 42). Similarly, induced expression of ALK variants results in increased cell survival upon TNF-α challenge, with the exception of KIF5B-ALK which does not express detectable Serpin B4 protein (Figs. 2*E* and 6 *E*–*H*).

High levels of Serpin B4 expression in HeLa cells have also been reported to inhibit apoptosis induced by NK cells (14, 43). Since Serpin B4 has been reported to interfere with the cytotoxic activity of Granzyme M, we hypothesized that the increased levels of Serpin B4 protein observed in EML4-ALK-V3 and TFG-ALK expressing cells may confer an increased resistance to NK cells. To test this hypothesis, we co-cultured ALK fusion expressing NL20 cells with polyclonally activated NK cells (Fig. 7*A*). In agreement with our hypothesis, induced EML4-ALK-V3 and TFG-ALK expressing cells, which robustly express Serpin B4, showed significantly reduced levels of apoptosis after co-culture with NK cells (Fig. 7*B*). In contrast, KIF5B-ALK and EML4-ALK-V1 expressing NL20 cells that fail to induce robust Serpin B4 protein production exhibited similar rates of apoptosis when co-cultured with NK cells as the uninduced NL20 line (Fig. 7*B*). To test the importance of Serpin B4 in the observed survival to NK cell-mediated cell death, we generated four independent Clustered regularly interspaced short palindromic repeats (CRISPR) deleted *SERPINB4* TFG-ALK NL20 (Fig. 7*C*) and three independent EML4-ALK-V3 NL20 cell clones (Fig. 7*E*). Three out of four doxycycline-induced knockout (KO) *SERPINB4* TFG-ALK cell clones and two out of three EML4-ALK-V3 NL20 cell clones exhibited increased

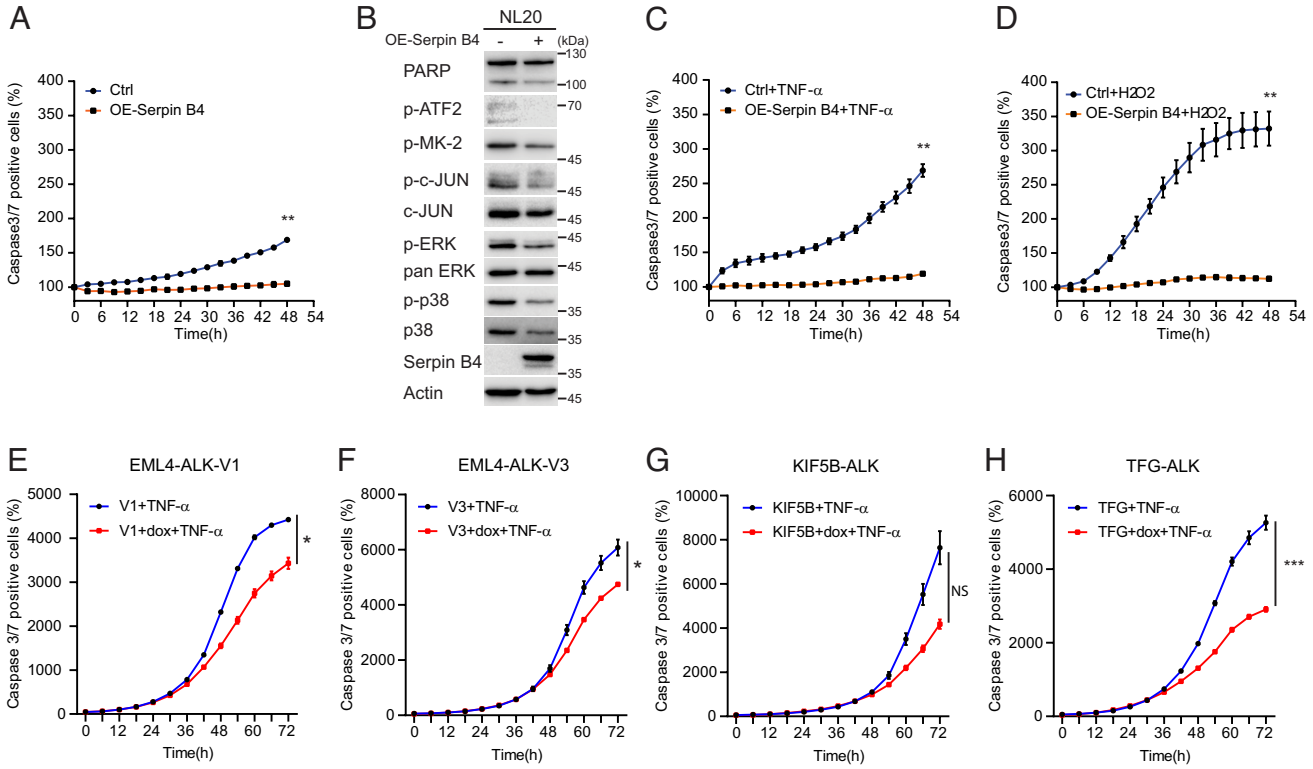

Fig. 6. Serpin B4 expression protects NL20 cells against apoptosis. (*A*) NL20 cells were transfected with either *pcDNA3-SERPINB4* or *pcDNA3* (Ctrl) for 24 h, after which cells were replated in 96-well plates and caspase-3/7 positive cell percentages were calculated and normalized using an IncuCyte® Live Cell Analysis system. Each data point represents mean ± SEM of normalized percentage conducted in triplicate (**$P < 0.01$; two-tailed paired *t* test). One typical experiment of three independent experiments is shown. (*B*) Lysates of NL20 cells transfected with either *pcDNA3-SERPINB4* or *pcDNA3* as control were collected after 48 h and subjected to immunoblotting with poly-ADP ribose polymerase (PARP), p-ATF2, p-MK-2, p-c-JUN, c-JUN, p-ERK1/2, pan-ERK, p-p38, p38, Serpin B4, and Actin antibodies as indicated. (*C* and *D*) NL20 cells were transfected with either *pcDNA3-SERPINB4* or *pcDNA3* (Ctrl) for 24 h followed by TNF-α (100 ng/mL) or H_2O_2 (0.05 M) treatment. Caspase-3/7 positive cell percentages were calculated and normalized using an IncuCyte® Live Cell Analysis system. Each data point represents mean ± SEM of normalized percentage, conducted in triplicate (**$P < 0.01$; two-tailed paired *t* test). One typical experiment of three independent experiments is shown. (*E*–*H*) ALK fusion cell lines, EML4-ALK-V1 (*E*), EML4-ALK-V3 (*F*), KIF5B-ALK (*G*), and TFG-ALK (*H*) in the presence or absence of doxycycline (dox), were treated with TNF-α (100 ng/mL). Caspase-3/7 positive cell percentages were calculated and normalized using an IncuCyte® Live Cell Analysis system. Each data point represents mean ± SEM of normalized percentage conducted in triplicate (NS, non-significant; *$P < 0.05$; ***$P < 0.001$; two-tailed paired *t* test). One typical experiment of three independent experiments is shown.

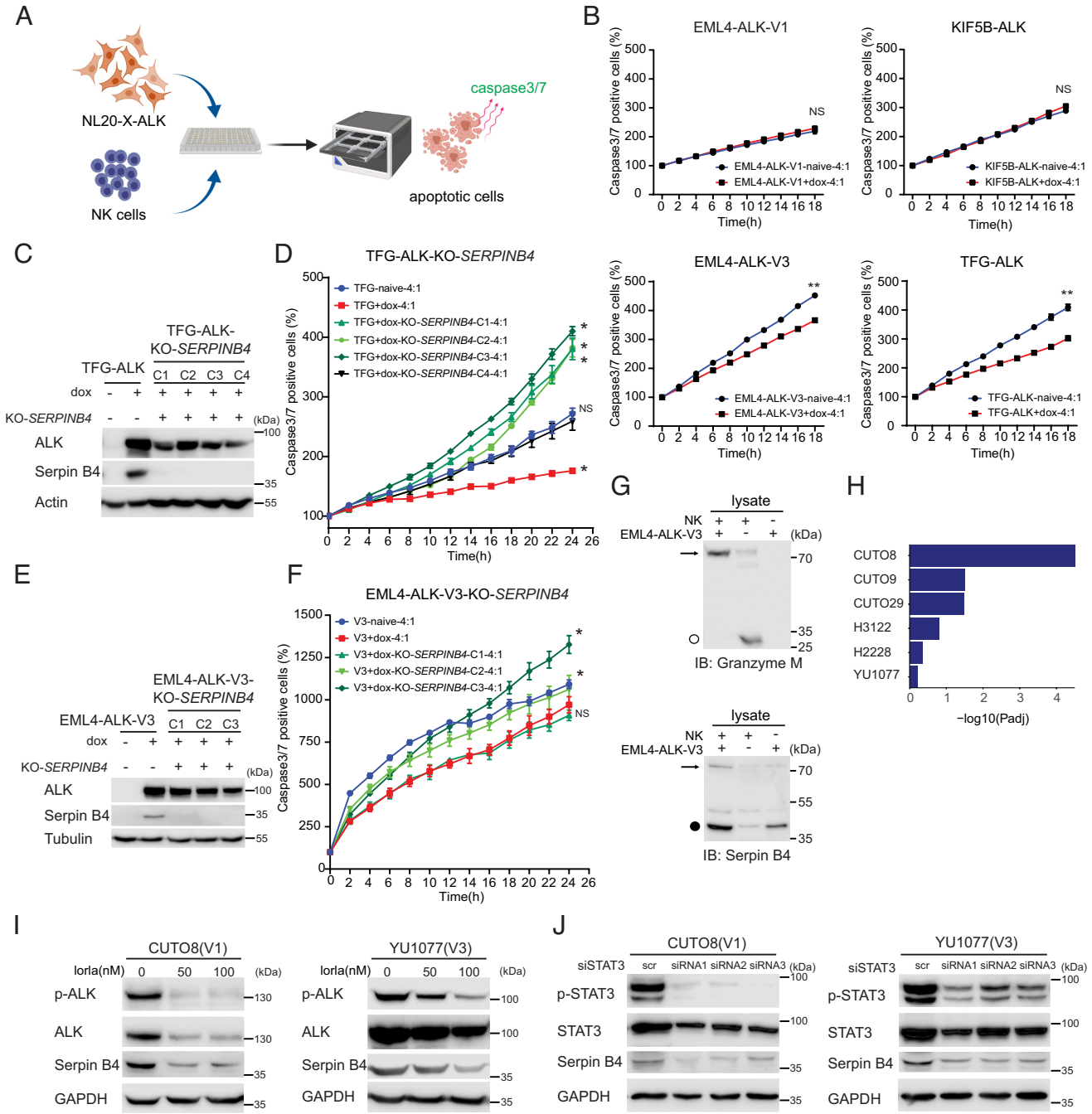

Fig. 7. Serpin B4 expression rescues ALK expressing NL20 cells from NK cell-mediated cytotoxicity. (*A*) Schematic outline of the NK cell and NL20-ALK cell co-culture assay employed. NL20-ALK cells were primed with doxycycline for 2 d, prior to incubation with NK cells. Incucyte® Caspase-3/7 Dye was used as an indicator for cells undergoing apoptosis. Apoptotic signals (green fluorescence) were analyzed by an IncuCyte® Live Cell Analysis system. (*B*) NL20-ALK cells primed with doxycycline for 2 d were incubated with NK cells at an effector to target cell ratio (E:T) of 4:1. Caspase-3/7 positive cell percentages were calculated and normalized to 0 h using an IncuCyte® Live Cell Analysis system. Each data point represents mean ± SEM of normalized percentage conducted in triplicate (NS, non-significant; $^{**}P < 0.01$; two-tailed paired *t* test). One typical experiment of three independent experiments is shown. (*C*) Immunoblotting analysis of Serpin B4 protein expression in parental NL20-TFG-ALK and four independent *SERPINB4* CRISPR/CRISPR associated protein 9 (Cas9)-engineered KO clones (C1 to C4). Cell lysates were immunoblotted with ALK, Serpin B4, and Actin antibodies as indicated. (*D*) *SERPINB4* KO NL20-TFG-ALK (C1 to C4) and parental control cells were primed with doxycycline (dox) for 2 d prior to co-culturing with NK cells and an E:T ratio of 4:1 and the percentage of caspase-3/7 positive cells calculated. Each data point represents mean ± SEM of normalized percentage conducted in triplicate (NS, non-significant; $^{*}P < 0.01$; two-tailed paired *t* test). One typical experiment of three independent experiments is shown. (*E*) Immunoblotting analysis of Serpin B4 protein expression in parental NL20-EML4-ALK-V3 and three independent *SERPINB4* CRISPR/Cas9-engineered KO clones (C1 to C3). Cell lysates were immunoblotted with ALK, Serpin B4, and Tubulin antibodies as indicated. (*F*) *SERPINB4* KO NL20-EML4-ALK-V3 (C1 to C3) and parental control cells were primed with doxycycline (dox) for 2 d prior to co-culturing with NK cells and an E:T ratio of 4:1 and the percentage of caspase-3/7 positive cells calculated. Each data point represents mean ± SEM of normalized percentage conducted in triplicate (NS, non-significant; $^{*}P < 0.01$; two-tailed paired *t* test). One typical experiment of three independent experiments is shown. (*G*) Immunoblotting analysis of co-incubated NK-92 and NL20-EML4-ALK-V3 lysates using Granzyme M and Serpin B4 antibodies indicates expression of Granzyme M (○, 27.5 kDa) in NK-92 cell lysates and Serpin B4 (●, 45 kDa) in NL20-EML4-ALK-V3 cell lysates. The formation of a Serpin B4 and Granzyme M complex (72.5 kDa) in the co-incubated lysates is indicated with an arrow. (*H*) Gene set enrichment for 27 inflammatory response genes (35) in DE genes in patient-derived cell lines treated with lorlatinib as indicated. GSEA was performed using Fisher's exact test. Bars represent P_{adj} values (−log10 scale). (*I*) CUTO8 and YU1077 were treated with lorlatinib (50 or 100 nM), and lysates were immunoblotted with pY1278-ALK, pan-ALK, Serpin B4, and GAPDH as indicated. Phospho-ALK was employed as readout of ALK inhibition. (*J*) CUTO8 and YU1077 cells were transfected with either control siRNA (scr) or siRNAs (1 to 3) targeting STAT3. Cell lysates were immunoblotted with pY705-STAT3, pan-STAT3, Serpin B4, and GAPDH antibodies as indicated.

levels of apoptosis compared with native Serpin B4 expressing cells after exposure to NK cells (Fig. 7 *D* and *F*).

To confirm the binding of Serpin B4 and Granzyme M, we co-incubated lysates from NL20-EML4-ALK-V3 cells treated with doxycycline, which express Serpin B4 (MW 45 kDa), and NK-92 cells, which express Granzyme M (MW 27.5 kDa), followed by immunoblotting analysis. Interaction of Serpin B4 and Granzyme M is predicted to result in the formation of a Serpin B4:Granzyme M complex of approximately 72.5 kDa on co-incubation of lysates. NK cells exhibited a predominantly unbound Granzyme M monomer at approximately 27.5 kDa as well as a weak band representing complex formation with endogenous Serpin B4 (Fig. 7*G*). Co-incubation of NL20-EML4-ALK-V3 cell lysates with NK cell lysates resulted in a Serpin B4:Granzyme M complex of approximately 72.5 kDa, indicating that Serpin B4 in NL20-EML4-ALK-V3 cells binds to Granzyme M produced by NK cells and suggests that the activity of Granzyme M may be inhibited as a result. Together, these data indicate that ALK fusion protein-driven *SERPINB4* expression in NL20 cells functions to inhibit NK cell-mediated cell death.

EML4-ALK-V1 and V3 Induce *SERPINB4* Expression via STAT3 in Patient-Derived Cell Lines. In agreement with our observations in NL20-ALK cell lines, we also observed significant enrichment of the inflammatory signature in ALK-positive NSCLC patient-derived cell lines (Fig. 7*H*). To determine whether ALK fusion activity regulates the expression of Serpin B4, CUTO8 (EML4-ALK-V1) and YU1077 (EML4-ALK-V3) cells were treated with lorlatinib. This resulted in decreased Serpin B4 expression in both cell lines at 72 h (Fig. 7*I*). Further, we observed a clear reduction in the phosphorylation of FOSL1, c-JUN, and STAT3 on ALK inhibition (*SI Appendix*, Fig. S8). We further investigated the importance of STAT3 for Serpin B4 expression in CUTO8 and YU1077 cells and observed that siRNA-mediated knockdown of STAT3 resulted in the loss of Serpin B4 (Fig. 7*J*). Thus, Serpin B4 expression also appears to be regulated by the ALK-STAT3 signaling axis in NSCLC patient-derived cell lines.

Discussion

In this work, we have developed a controlled NL20-based bronchial epithelial cell system expressing four different oncogenic ALK fusions found in NSCLC, aiming to identify additional molecular mechanisms relevant to ALK-positive NSCLC. Our characterization confirms previous findings that EML4-ALK-V1 and KIF5B protein, which exhibit longer fusion partners (Fig. 1*A*), were less stable than EML4-ALK-V3 and TFG-ALK, which have shorter fusion partners (22, 23). Our experimental model also confirmed the observation that KIF5B-ALK exhibits the highest level of in vitro kinase activity (22).

We performed extensive RNA-seq and phosphoproteomics analysis in this panel of inducible ALK fusion cell lines in the presence and absence of ALK TKI treatment. In addition to identification of the previously reported ALK tyrosine phosphorylation sites (1, 26–29), we noted several differentially phosphorylated sites, such as Y1359, which was lorlatinib sensitive on EML4-ALK-V1, EML4-ALK-V3, and KIF5B-ALK but not on TFG-ALK. ALK Y1131 also showed different degrees of phosphorylation between the ALK fusion variants. Although we could detect differences in the phosphorylation status of phosphotyrosine binding domains (SH2 and PTB) containing proteins downstream of the four ALK fusions suggesting a differential signaling output, we were unable to correlate these with previously identified binding proteins at these sites, such as PI3K and PLC-γ. Therefore, the overall effect of these differential ALK phosphorylation patterns on downstream signaling is unclear at this time. Another consideration is the differential stabilities and subcellular localizations of the EML4-ALK, KIF5B-ALK, and TFG-ALK fusions that vary dependent on the ALK fusion partner and which we have not been addressed in this study. Understanding the differences in the downstream signaling output from the downstream ALK fusions will require further experimental analysis.

Our initial RNA-seq analysis identified an inflammatory signature that was shared upon induction of all four ALK fusions variants. This included a robust expression of the *SERPINB* family of serine protease inhibitors, which are clustered at chr.18q21 (12, 13). *SERPINB4* expression has previously been described as regulated downstream of oncogenes such as Ras (44). Our findings here suggest that STAT3, which is a major tyrosine phosphorylation target of the various NSCLC ALK fusions (EML4-ALK-V1, EML4-ALK-V3, TFG-ALK, and KIF5B-ALK), is also important for the expression of *SERPINB4*. Interestingly, previous ChIP analyses have reported binding of STAT3 to the *SERPINB4* promoter (34), in support of our findings here. We also identified potential NF-κB binding sites in the promoter region of the *SERPINB4* gene, as well as an effect of NF-κB pathway inhibition on *SERPINB4* expression downstream of oncogenic ALK fusions. The mechanism by which the ALK fusion proteins activate NF-κB signaling is not clear; however, the striking tyrosine phosphorylation both NF-κB1 and NF-κB2 downstream of the various ALK fusions suggests they may be directly implicated. To our knowledge, tyrosine phosphorylation of NF-κB downstream of oncogenic ALK fusions has not been reported in any cancer. The mechanism underlying this will require further investigation; however, both NF-κB1 (p105) and NF-κB2 (p100) tyrosine phosphorylation sites observed here (Tyr 81 and Tyr 77) are located in the N-terminal p50/p52 subunits of NF-κB1/NF-κB2, respectively, within the Rel-homology domain, responsible for DNA binding and dimerization (45, 46). Investigation of public datasets show that Tyr 77 phosphorylation of NF-κB1 has previously been observed, although not further investigated, in the ALK-positive H3122 and H2228 NSCLC cell lines (www.phosphosite.org). Tyrosine's 77 and 81 and their surrounding amino acids are highly conserved from mouse to humans, suggesting that these sites may have functional relevance. Further support for a functional significance of Tyr 77 and Tyr 81 phosphorylation comes from a recent report in which TNF-α-induced Ser 80 phosphorylation of NF-κB1 by IKKβ was shown to impact on DNA binding and transcription (47). In addition, Abate and colleagues reported a strong NF-κB signature while characterizing a TRAF1-ALK fusion-driven ALCL patient-derived cell line, suggesting that inappropriate ALK activation may drive NF-κB pathways (48). Here we note that while a robust phosphorylation of Tyr 77 and 81 was observed, and we could show that this was abrogated in the presence of lorlatinib, we did not observe any resultant cleavage of either NF-κB1 or NF-κB2 downstream of ALK. Whether ALK fusion-driven tyrosine phosphorylation of NF-κB regulates nuclear translocation or DNA binding and transcription remains to be resolved.

Recently, it was shown that Serpin B9 protects various cancer cells from their own production of Granzyme B and for the tumor cell survival and for the presence of immunosuppressive cells in the tumor microenvironment (49). Further, overexpression of Serpin B4 in cells inhibits recombinant Granzyme M as well as NK cell-mediated cell death. Serpin B4 has the ability to abrogate the proteolytic activity of Granzyme M toward natural substrate (14, 38). Similarly, we observed an increased cell survival upon overexpression of *SERPINB4* in parental NL20 cells when challenged with TNF-α or with hydrogen peroxide (H_2O_2), suggesting that *SERPINB4* expression suppresses cell death.

Our work here shows that the TFG-ALK and EML4-ALK-V3 fusion proteins transcriptionally regulate *SERPINB* family expression. We also show that *SERPINB4* expression improves cell survival and reduces NK mediated cytotoxicity. Further, CRISPR/Cas9-mediated KO of *SERPINB4* in TFG-ALK and EML4-ALK-V3 KO cells results in increased NK cell-mediated cytotoxicity, suggesting this may be physiologically relevant in vivo. Importantly, we show Serpin B4 expressed by NL20 cells forms a physical complex with Granzyme M expressed by NK cells, providing mechanistic support for this hypothesis.

Our findings in ALK fusion expressing NL20 cells are further supported in cell lines derived from NSCLC patients, such as H2228, H3122, and the recently characterized CUTO8, CUTO9, CUTO29, and YU1077 cells (24). In those NSCLC lines expressing EML4-ALK-V3, expression of *SERPINB4* is dramatically decreased upon inhibition of ALK activity with lorlatinib. In contrast, CUTO8, CUTO9, and H3122, which express the more unstable EML4-ALK-V1 fusion, express lower levels of Serpin B4 proteins. Finally, since Serpin B4 is highly expressed by EML4-ALK-V3 and TFG-ALK NL20 and patient-derived NSCLC cell lines, our results suggest a novel mechanism by which ALK fusion positive tumor cells evade cytotoxic lymphocyte-induced Granzyme M-mediated cell death. This mechanism may contribute to the decreased progression-free survival and overall response rate observed in NSCLC patients harboring EML4-ALK-V3 when compared with EML4-ALK-V1 patients.

Materials and Methods

NL20 cells expressing four different inducible ALK fusion variants found in NSCLC (EML4-ALK-V1, -V3, KIF5B-ALK, and TFG-ALK) were generated. The different ALK fusions were characterized immunoprecipitation and immunoblotting analyses employing validated antibodies and for cell growth with an IncuCyte live cell system. In-depth analysis of the effect of the various ALK fusion included RNA-seq and phosphoproteome analyses in the presence or absence of ALK inhibitors. NL20 cells overexpressing SERPINB4 together with *SERPINB4* KO CRISPR cells were generated and investigated for proliferation, immunoprecipitation, and immunoblotting analyses employing validated antibodies. Cells were further investigated by mouse xenografts and in parallel by co-culturing with NK cells prior to analysis for caspase activity employing an IncuCyte live cell system. Statistical, data, and gene set enrichments analyses were performed with two-sample *t* tests (GraphPad Prism), employing Benjimini–Hochberg method and DEseq2 statistic, respectively. Detailed *Materials and Methods* and data analysis information are supplied in the *SI Appendix*.

Data, Materials, and Software Availability. RNA-seq data and Phosphoproteomics data have been deposited in ArrayExpress and ProteomeXchange Consortium. RNA-seq data have been deposited to ArrayExpress with the accession numbers: E-MTAB-11304 (https://www.ebi.ac.uk/arrayexpress/experiments/E-MTAB-11304) (50); E-MTAB-11342 (https://www.ebi.ac.uk/arrayexpress/experiments/E-MTAB-11342) (51); E-MTAB-11834 (https://www.ebi.ac.uk/arrayexpress/experiments/E-MTAB-11834) (52). The mass spectrometry proteomics data have been deposited to the ProteomeXchange Consortium (http://proteomecentral.proteomexchange.org) via the PRIDE partner repository (53) with the dataset identifier PXD035100. All other data required to evaluate the conclusions in the paper are provided in Supplementary Materials. Source code available at GitHub https://github.com/CCGGlab/ALK_fusion (54). All results are also available in an interactive web application at https://ccgg.ugent.be/shiny/alk_fusion_2023/.

ACKNOWLEDGMENTS. This work has been supported by grants from the Sjöberg Foundation (2017-12-22), Swedish Cancer Society (B.H.: CAN21/1525; R.H.P. CAN21/1459), the Swedish Research Council (R.H.P.: 2019-03914; B.H.:2021-01192), and Ghent University Special Research Fund (BOF) Starting Grant (J.V.d.E.: BOF.STG.2019.0073.01).

Author affiliations: [a]Department of Medical Biochemistry and Cell Biology, Institute of Biomedicine, Sahlgrenska Academy, Gothenburg University, 40530 Gothenburg, Sweden; [b]Department of Human Structure and Repair, Anatomy and Embryology Unit, Ghent University, 9000 Ghent, Belgium; [c]Department of Respiratory Medicine, Sahlgrenska University Hospital, 41345 Gothenburg, Sweden; and [d]Division of Medical Oncology, University of Colorado School of Medicine, Aurora, CO 80045

1. K. Rikova *et al.*, Global survey of phosphotyrosine signaling identifies oncogenic kinases in lung cancer. *Cell* **131**, 1190–1203 (2007).
2. M. Soda *et al.*, Identification of the transforming EML4-ALK fusion gene in non-small-cell lung cancer. *Nature* **448**, 561–566 (2007).
3. S. I. Ou, V. W. Zhu, M. Nagasaka, Catalog of 5′ fusion partners in ALK-positive NSCLC Circa 2020. *JTO Clin. Res. Rep.* **1**, 100015 (2020).
4. J. J. Lin *et al.*, Impact of EML4-ALK variant on resistance mechanisms and clinical outcomes in ALK-positive lung cancer. *J. Clin. Oncol.* **36**, 1199–1206 (2018).
5. S. S. Zhang, M. Nagasaka, V. W. Zhu, S. I. Ou, Going beneath the tip of the iceberg. Identifying and understanding EML4-ALK variants and TP53 mutations to optimize treatment of ALK fusion positive (ALK+) NSCLC. *Lung Cancer* **158**, 126–136 (2021).
6. F. Armstrong *et al.*, Differential effects of X-ALK fusion proteins on proliferation, transformation, and invasion properties of NIH3T3 cells. *Oncogene* **23**, 6071–6082 (2004).
7. T. Yoshida *et al.*, Differential crizotinib response duration among ALK fusion variants in ALK-positive non-small-cell lung cancer. *J. Clin. Oncol.* **34**, 3383–3389 (2016).
8. P. Christopoulos *et al.*, EML4-ALK fusion variant V3 is a high-risk feature conferring accelerated metastatic spread, early treatment failure and worse overall survival in ALK(+) non-small cell lung cancer. *Int. J. Cancer* **142**, 2589–2598 (2018).
9. P. Christopoulos *et al.*, Identification of a highly lethal V3(+)TP53(+) subset in ALK(+) lung adenocarcinoma. *Int. J. Cancer* **144**, 190–199 (2019).
10. D. R. Camidge *et al.*, Brigatinib versus crizotinib in ALK inhibitor-naive advanced ALK-positive NSCLC: Final results of phase 3 ALTA-1L trial. *J. Thorac. Oncol.* **16**, 2091–2108 (2021).
11. C. Heit *et al.*, Update of the human and mouse SERPIN gene superfamily. *Hum. Genom.* **7**, 22 (2013).
12. M. Shiiba *et al.*, Down-regulated expression of SERPIN genes located on chromosome 18q21 in oral squamous cell carcinomas. *Oncol. Rep.* **24**, 241–249 (2010).
13. Y. Sun, N. Sheshadri, W. X. Zong, SERPINB3 and B4: From biochemistry to biology. *Semin Cell Dev. Biol.* **62**, 170–177 (2017).
14. P. J. de Koning *et al.*, Intracellular serine protease inhibitor SERPINB4 inhibits granzyme M-induced cell death. *PLoS One* **6**, e22645 (2011).
15. S. A. de Poot, N. Bovenschen, Granzyme M: Behind enemy lines. *Cell Death Differ.* **21**, 359–368 (2014).
16. G. Urquhart *et al.*, Serpin b3 is associated with poor survival after chemotherapy and is a potential novel predictive biomarker in advanced non-small-cell lung cancer. *J. Thorac. Oncol.* **8**, 1502–1509 (2013).
17. N. Riaz *et al.*, Recurrent SERPINB3 and SERPINB4 mutations in patients who respond to anti-CTLA4 immunotherapy. *Nat. Genet.* **48**, 1327–1329 (2016).
18. C. E. McCoach *et al.*, Resistance mechanisms to targeted therapies in ROS1(+) and ALK(+) non-small cell lung cancer. *Clin. Cancer Res.* **24**, 3334–3347 (2018).
19. Y. Amano *et al.*, Oncogenic TPM3-ALK activation requires dimerization through the coiled-coil structure of TPM3. *Biochem. Biophys. Res. Commun.* **457**, 457–460 (2015).
20. Y. L. Choi *et al.*, A novel fusion of TPR and ALK in lung adenocarcinoma. *J. Thorac. Oncol.* **9**, 563–566 (2014).
21. K. Takeuchi *et al.*, Multiplex reverse transcription-PCR screening for EML4-ALK fusion transcripts. *Clin. Cancer Res.* **14**, 6618–6624 (2008).
22. M. A. Childress *et al.*, ALK fusion partners impact response to ALK inhibition: Differential effects on sensitivity, cellular phenotypes, and biochemical properties. *Mol. Cancer Res. MCR* **16**, 1724–1736 (2018).
23. J. M. Heuckmann *et al.*, Differential protein stability and ALK inhibitor sensitivity of EML4-ALK fusion variants. *Clin. Cancer Res.* **18**, 4682–4690 (2012).
24. A. A. Bokhari *et al.*, Novel human-derived EML4-ALK fusion cell lines identify ribonucleotide reductase RRM2 as a target of activated ALK in NSCLC. *Lung Cancer* **171**, 103–114 (2022).
25. D. Chand *et al.*, Cell culture and Drosophila model systems define three classes of anaplastic lymphoma kinase mutations in neuroblastoma. *Dis. Model. Mech.* **6**, 373–382 (2013).
26. K. B. Emdal *et al.*, Integrated proximal proteomics reveals IRS2 as a determinant of cell survival in ALK-driven neuroblastoma. *Sci. Signaling* **11**, eaap9752 (2018).
27. K. Sattu *et al.*, Phosphoproteomic analysis of anaplastic lymphoma kinase (ALK) downstream signaling pathways identifies signal transducer and activator of transcription 3 as a functional target of activated ALK in neuroblastoma cells. *FEBS J.* **280**, 5269–5282 (2013), 10.1111/febs.12453.
28. J. Van den Eynden *et al.*, Phosphoproteome and gene expression profiling of ALK inhibition in neuroblastoma cell lines reveals conserved oncogenic pathways. *Sci. Signal.* **11**, eaar5680 (2018).
29. G. Zhang *et al.*, Coupling an EML4-ALK-centric interactome with RNA interference identifies sensitizers to ALK inhibitors. *Sci. Signal.* **9**, rs12 (2016).
30. J. Guan *et al.*, Novel mechanisms of ALK activation revealed by analysis of the Y1278S neuroblastoma mutation. *Cancers (Basel)* **9**, 149 (2017).
31. C. J. Tartari *et al.*, Characterization of some molecular mechanisms governing autoactivation of the catalytic domain of the anaplastic lymphoma kinase. *J. Biol. Chem.* **283**, 3743–3750 (2008).
32. C. C. Lee *et al.*, Crystal structure of the anaplastic lymphoma kinase (ALK) catalytic domain. *Biochem. J.* **430**, 425–437 (2010).
33. R. T. Bossi *et al.*, Crystal structures of anaplastic lymphoma kinase in complex with ATP competitive inhibitors. *Biochemistry* **49**, 6813–6825 (2010).

34. S. T. Ahmed, J. E. Darnell Jr., Serpin B3/B4, activated by STAT3, promote survival of squamous carcinoma cells. *Biochem. Biophys. Res. Commun.* **378**, 821–825 (2009).
35. Z. Ji, L. He, A. Regev, K. Struhl, Inflammatory regulatory network mediated by the joint action of NF-kB, STAT3, and AP-1 factors is involved in many human cancers. *Proc. Natl. Acad. Sci. U.S.A.* **116**, 9453–9462 (2019).
36. D. Guo, J. D. Dunbar, C. H. Yang, L. M. Pfeffer, D. B. Donner, Induction of Jak/STAT signaling by activation of the type 1 TNF receptor. *J. Immunol.* **160**, 2742–2750 (1998).
37. C. Miao *et al.*, Perfluorooctanoic acid enhances colorectal cancer DLD-1 cells invasiveness through activating NF-kappaB mediated matrix metalloproteinase-2/-9 expression. *Int. J. Clin. Exp. Pathol.* **8**, 10512–10522 (2015).
38. M. H. Shamji *et al.*, Antiapoptotic serine protease inhibitors contribute to survival of allergenic TH2 cells. *J. Allergy Clin. Immunol.* **142**, 569–581.e565 (2018).
39. A. Murakami *et al.*, Squamous cell carcinoma antigen suppresses radiation-induced cell death. *Br. J. Cancer* **84**, 851–858 (2001).
40. C. Katagiri, J. Nakanishi, K. Kadoya, T. Hibino, Serpin squamous cell carcinoma antigen inhibits UV-induced apoptosis via suppression of c-JUN NH2-terminal kinase. *J. Cell Biol.* **172**, 983–990 (2006).
41. A. S. Dhillon, S. Hagan, O. Rath, W. Kolch, MAP kinase signalling pathways in cancer. *Oncogene* **26**, 3279–3290 (2007).
42. A. F. McGettrick, R. C. Barnes, D. M. Worrall, SCCA2 inhibits TNF-mediated apoptosis in transfected HeLa cells. The reactive centre loop sequence is essential for this function and TNF-induced cathepsin G is a candidate target. *Eur. J. Biochem.* **268**, 5868–5875 (2001).
43. A. Takeda, A. Kajiya, A. Iwasawa, Y. Nakamura, T. Hibino, Aberrant expression of serpin squamous cell carcinoma antigen 2 in human tumor tissues and cell lines: Evidence of protection from tumor necrosis factor-mediated apoptosis. *Biol. Chem.* **383**, 1231–1236 (2002).
44. J. M. Catanzaro *et al.*, Oncogenic Ras induces inflammatory cytokine production by upregulating the squamous cell carcinoma antigens SerpinB3/B4. *Nat. Commun.* **5**, 3729 (2014).
45. K. Taniguchi, M. Karin, NF-kappaB, inflammation, immunity and cancer: Coming of age. *Nat. Rev. Immunol.* **18**, 309–324 (2018).
46. M. R. Zinatizadeh *et al.*, The Nuclear Factor Kappa B (NF-kB) signaling in cancer development and immune diseases. *Genes. Dis.* **8**, 287–297 (2021).
47. E. L. Smith *et al.*, The regulation of sequence specific NF-kappaB DNA binding and transcription by IKKbeta phosphorylation of NF-kappaB p50 at serine 80. *Nucleic Acids Res.* **47**, 11151–11163 (2019).
48. F. Abate *et al.*, A novel patient-derived tumorgraft model with TRAF1-ALK anaplastic large-cell lymphoma translocation. *Leukemia* **29**, 1390–1401 (2015).
49. L. Jiang *et al.*, Direct tumor killing and immunotherapy through anti-SerpinB9 therapy. *Cell* **183**, 1219–1233.e1218 (2020).
50. T. Chuang *et al.*, Data from "ALK fusion NSCLC oncogenespromote survival and inhibit NK cell responses via SERPINB4 expression". *ArrayExpress:* https://www.ebi.ac.uk/arrayexpress/experiments/E-MTAB-11304. Deposited January 14, 2022.
51. T. Chuang *et al.*, Data from "ALK fusion NSCLC oncogenespromote survival and inhibit NK cell responses via SERPINB4 expression". *ArrayExpress:* https://www.ebi.ac.uk/biostudies/arrayexpress/studies/E-MTAB-11834. Deposited June 17, 2022.
52. A. A. Bokhari *et al.*, Data from "Novel human-derived EML4-ALK fusion cell lines identify ribonucleotide reductase RRM2 as a target of activated ALK in NSCLC". https://www.ebi.ac.uk/arrayexpress/experiments/E-MTAB-11342. Deposited January 21, 2022.
53. Y. Perez-Riverol *et al.*, The PRIDE database resources in 2022: a hub for mass spectrometry-based proteomics evidences. *Nucleic Acids Res.* **50**(D1): D543-D552. 10.1093/nar/gkab1038. PMID: 34723319; PMCID: PMC8728295. 2022 Jan 7
54. T. Chuang *et al.*, Data from "ALK fusion NSCLC oncogenes promote survival and inhibit NK cell responses via SERPINB4 expression". *Github:* https://github.com/CCGGlab/ALK_fusion. Available January 25, 2023.